CHARACTERIZATION OF ALTERED AND MINIMALLY ALTERED BASALTIC GLASSES USING VISIBLE-THERMAL INFRARED SPECTROSCOPY, X-RAY DIFFRACTION, AND RAMAN SPECTROSCOPY. W.H. Farrand[1], S.P. Wright[2], and T.D. Glotch[3]. [1]Space Science Institute, 4750 Walnut St., #205, Boulder, CO 80301, farrand@spacescience.org, [2]Planetary Science Institute, Tucson, AZ 85719, [3]Department of Geosciences, Stony Brook University, Stony Brook, NY 11794.

Introduction: The exploration of the Martian surface by the rovers Spirit, Opportunity, and Curiosity has indicated the widespread presence of clastic rocks of basaltic composition [1-3], many of which have altered to various extents. In this investigation, we have examined basaltic ash and tephra formed through hydrovolcanism (the explosive interaction of magma with liquid water), glaciovolcanism (eruptions occurring below ice sheets), and impact processes (at the Lonar Crater in India [4-5]). We have utilized several analysis techniques available to the Mars Exploration Rovers and the Mars Science Laboratory rover. In particular, we have focused on VNIR reflectance and TIR emittance spectroscopy. We have performed standard thin section petrography and have utilized supporting X-ray diffraction (XRD) and Raman spectroscopy measurements.

Alteration: Alteration of basaltic glass can occur under ambient temperatures over long time spans through the process of pedogenesis [6]. Alteration may occur more rapidly through hydrothermal alteration or nearly syndepositionally through deposition with steam in the case of hydro- or glaciovolcanism [7]. Basaltic glass can also alter through burial diagenesis [8], although examples of this alteration pathway were not examined in this study. The hydrated and oxidized alteration product of basaltic glass is palagonite. Palagonite is recognized in all of these alteration pathways; however, the extent to which the glass is palagonitized in the latter alteration pathways led Schiffman et al. [6] to deem this form of alteration "palagonitic alteration".

Field Areas: We conducted field work at several hydrovolcanic eruption sites in Idaho, New Mexico, and Utah. Samples were collected by team members in past projects from glaciovolcanic sites in Washington state and Iceland. One of our team has also conducted extensive field work at Lonar Crater [e.g., 5]. Several sample of ambiently weathered basaltic ash collected by one of us from the summit of the Haleakala volcano were also examined.

Analysis: Thin sections were made of a number of field samples for optical petrography. Powdered samples (ground to less than a 400 μm mesh size) were sent to the RELAB facility at Brown University to have their 0.3 – 2.6 μm bidirectional and 0.83 – 25 μm biconical reflectance measured. MWIR emissivity of a number of samples was measured at Arizona State University, Stony Brook University, and the Southwest Research Institute. XRD analysis of samples was conducted at Auburn University and Raman spectroscopic analysis of several samples was conducted at the Geomicrobiology Laboratory at the University of Colorado and a number of thin sections were also examined using the micro-FTIR reflectance spectrometer at the Stony Brook University Vibrational Spectroscopy Laboratory.

VNIR Reflectance Spectroscopy: Bidirectional reflectance spectra were examined over the 0.3 to 2.6 μm and 3 to 6 μm ranges of 52 samples including minimally altered gray tuffs, orange-colored hydrovolcanic palagonite tuffs and glaciovolcanic palagonitized hyaloclastites, and orange-colored disaggregated palagonitic Haleakala soils. A clear distinction is observed between the gray tuffs, the hydro- and glaciovolcanic tuffs and the palagonitic soils. This is consistent with past studies of these and similar spectra [e.g., 9]. A more subtle distinction is observed between the hydrovolcanic palagonite tuffs and the glaciovolcanic palagonitized hyaloclastites over these two spectral ranges. One of the distinguishing features between these latter two sets of tephras is the presence of absorption features at 2.5 and 4.5 μm (**Fig. 1-2**) in the former, but not in the latter (or only weakly expressed in the latter). These bands are attributed to the presence of more zeolites in the hydrovolcanic palagonite tuffs versus the glaciovolcanic palagonitized hyaloclastites. The presence of zeolites in the hydrovolcanic palagonite tuffs was also confirmed through XRD analysis and Raman spectroscopy indicated a good match to chabazite of one of the zeolites.

The glaciovolcanic palagonitized hyaloclastites also show better development of a metal-OH overtone band. The hydrovolcanic palagonite tuffs display weak development of a band at 2.295 μm while the glaciovolcanic palagonitized hyaloclastites have a better expressed Al-OH band at 2.195 μm (**Fig. 1B**).

Detection of Glass in Thermal Emissivity Spectra: Ruff et al. [10] used a linear deconvolution approach to detect significant fractions of glass in Mini-TES spectra of Husband Hill and Home Plate rocks observed by the Spirit rover. However, minimal

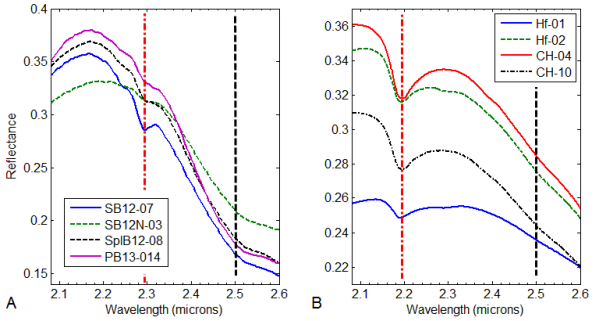

Fig. 1. Reflectance spectra over 2.1 to 2.6 μm range. **A**. Hydrovolcanic palagonite tuffs with 2.5 μm band indicated by black dashed line. Weak 2.29 μm band indicated by red dash-dot line. **B**. Lack of 2.5 μm band in glaciovolcanic tuffs indicated by black dashed line and 2.2 μm band indicated by red dash-dot line.

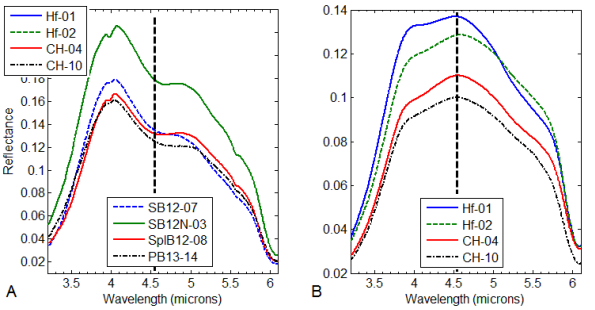

Fig. 2. Reflectance spectra over 3.2 to 6 μm range. **A**. 4.5 μm band in hydrovolcanic palagonite tuffs indicated by dashed black line. **B**. Glaciovolcanic palagonitized hyaloclastites with lack of 4.5 μm band indicated by dashed black line.

ly altered basaltic glass-rich tuffs produced in hydrovolcaniceruptions are not modeled as having as much glass as roughly equally glass-rich glaciovolcanic tuffs (**Fig. 3**). The glass-rich hydrovolcanic tuffs display more of a doublet feature near 1000 cm^{-1} than do the glass-rich glaciovolcanic tuffs with the latter thus more closely resembling a pure glass spectrum (**Fig. 4**).

Interestingly, there is a spectral similarity between the glass-rich glaciovolcanic Hf-06 spectrum and the glass-rich Lonar Class 5A spectrum [5] and also between the glass-rich hydrovolcanic NMB12-14 spectrum and the Lonar Class 5B spectrum [5] (**Fig. 4**). Due to their similar geochemistries, the difference in the two impact melt spectra [5] was suggested to be due to titanomagnetite crystallites in Class 5A (seen in BSE images) that reflect either incomplete shock-melting or a different alteration pathway. The similarity of the two impact melt spectra to the spectra of a hydrovolcanic and glaciovolcanic glass suggests that minute alteration mineralogy may be the reason. Investigating these four spectra (**Fig. 4**) and others will guide future analyses to determine the alteration mineralogy.

References: [1] Squyres S.W. et al. (2005) *JGR,111*, 10.1029/2005JE002562. [2] Squyres S.W. et al. (2012) *Science*, *336*, 570. [3] Vaniman D.T. et al. (2013) *Science*, *343*, DOI: 10.1126/science.1243480. [4] Fredriksson K. (1973) *Science*, *180*, 862. [5] Wright S.P. et al. (2011) *JGR*, *116*, 10.1029/2010JE003785. [6] Schiffman, P. et al. (2000) *G3*, *1*, 2000GC000068. [7] Wohletz K.H. and M.F. Sheridan (1983) *Am. J. Sci.*, *283*, 385. [8] Walton A.W. et al. (2005) *G3*, *6*, doi:10.1029/2004GC000903. [9] Farrand W.H. and Singer R.B. (1992) *JGR*, *97*, 17393. [10] Ruff S.W. et al. (2006) *JGR*, *111*, doi:10.1029/2006JE002747.

Acknowledgements: This work was funded through MFRP grant NNX12AH92G. Thanks to V. Hamilton of SWRI for TIR measurements and A. Templeton of the U. of Colorado for Raman measurements.

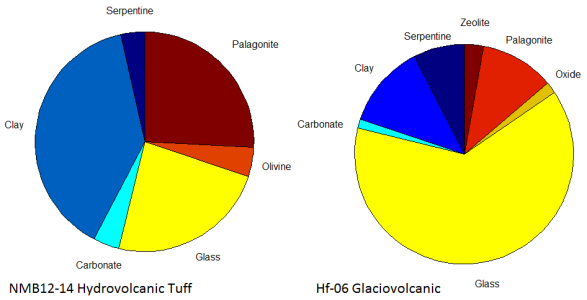

Fig. 3. Linear deconvolution results of approximately equally glass-rich hydrovolcanic tuff NMB12-14 and glaciovolcanic hyaloclastite Hf-06.

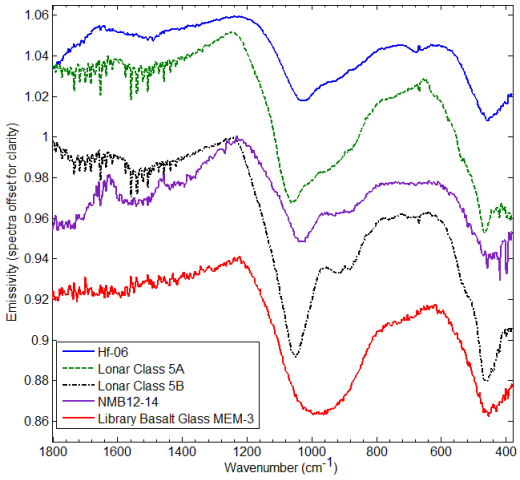

Fig. 4. Thermal emissivity spectra showing similarity of glassy glaciovolcanic hyaloclastite Hf-06 to Lonar Class 5A impact melt and of glassy hydrovolcanic tuff NMB12-14 to Lonar Class 5B melt with library glass MEM-3 for comparison.